Photochromism in Transition-Metal-Doped $SrTiO_3$ †

B. W. Faughnan
RCA Laboratories, Princeton, New Jersey 08540
(Received 21 December 1970)

The photochromic properties of transition-metal-doped $SrTiO_3$ are studied using optical and electron paramagnetic resonance techniques. In addition to the double doped systems containing Fe+Mo and Ni+Mo, which were treated briefly in earlier publications, the photochromic effect in $SrTiO_3$ singly doped with Ni, Fe, and Co is discussed in detail. The centers responsible for the photochromic absorption are identified, and the visible absorption bands are tied to specific transition metals in particular sites (axial or cubic) and oxidation states. It is found that when Mo is not present, a transition ion can act as both an electron donor and an electron trap. Models are proposed for the nature of the band-edge coloring absorption and the visible photochromic absorption bands.

I. INTRODUCTION

Photochromism, the reversible change in color of a material under light irradiation, has been observed in numerous organic and inorganic substances. Several reviews of the literature have been writen.[1-5] Many of the inorganic photochromic (PC) materials studied were minerals, and the color centers introduced were F centers formed by the trapping of electrons, released by uv irradiation, by vacancies already present in the crystal.[6,7] A classic example of PC behavior is the conversion of F into F' centers in alkali halides.[8-10] For most of these instances, with the exception of the above mentioned $F \rightarrow F'$ transition in alkali halides, the detailed physics of the process could not be worked out, nor could the relevant impurity centers be identified.

More recently, we have undertaken a detailed study of photochromism in transition-metal-doped $SrTiO_3$. It has been possible to identify, to a considerable degree, the centers responsible for this effect. Preliminary results have already been reported.[11,12] Cathodochromism, that is, coloration under electron-beam irradiation, has also been observed in these materials.[13] In this paper the results of a detailed study of the system $SrTiO_3$: TM (transition metal) are presented.

Interest in photochromic materials has increased recently because of their potential usefulness for memory and display devices. From a scientific point of view the charge-transfer type of absorption bands found in PC $SrTiO_3$ appear to have received little attention in the literature, in spite of the fact that their occurrence should be rather widespread. The study of these strong absorption bands should yield considerable understanding of the nature of a certain class of impurity centers in insulators.

In Sec. II, the model proposed for the PC effect in $SrTiO_3$, described in Ref. 10, is reviewed. In Sec. III, some experimental details are discussed, while the detailed experimental results are presented in Sec. IV. Section V treats the nature of the PC excitation and absorption in $SrTiO_3$, while in Sec. VI, the conclusions and a summary of the results are presented.

II. PC MODEL FOR TITANATES: GENERAL CHARACTERISTICS

$SrTiO_3$ is a crystal having the cubic perovskite structure at room temperature. This is shown in Fig. 1. A slight tetragonal distortion is introduced below the transition temperature of 107 °K, as can be seen by electron paramagnetic resonance (EPR) measurements.[14] All of the transition metals studied enter the lattice substitutionally on Ti^{4+} sites, as would be expected from ionic radii considerations. Other ions, for example, trivalent rare earths, can be substituted on the Sr sites but have no discernible effect on the photochromic properties, other than the obvious one of affecting charge compensation.

Charge compensation plays an important role in PC $SrTiO_3$, since it permits the existence of many different valence states of impurity ions in the crystal. One method of charge compensation consists of double doping the crystal with two impurities so that the charge unbalance of one impurity ion of the

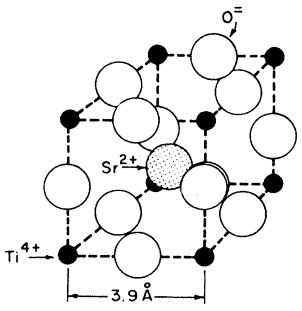

FIG. 1. Crystal structure of $SrTiO_3$.

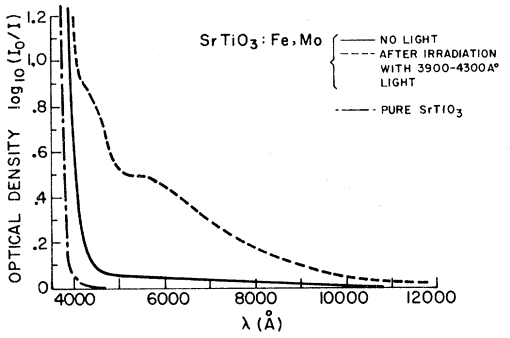

FIG. 2. Optical absorption in $SrTiO_3$: Fe, Mo before and after irradiation with 3900–4300-Å light. Sample thickness = 0.025 cm, $T = 77\,^{\circ}K$.

desired oxidation number or valence state is cancelled by another different suitably chosen ion. However, if the PC ion is deficient in positive charge relative to Ti^{4+}, e.g., Fe^{3+}, Ni^{2+}, etc., charge compensation can result from oxygen vacancies. The ease with which oxygen vacancies can be introduced or removed by impurity doping and heat treatment (oxidation reduction) is an important property which can be utilized to place all impurity ions in the desired valence state. It is also a useful technique for understanding the PC mechanism.

$SrTiO_3$, with a band gap of approximately 3.2 eV, is transparent in the visible. When doped with Fe or other transition metals, a small amount of visible absorption appears. This usually takes the form of a smearing out of the band edge so that some absorption is now in the blue end of the visible spectrum. In some cases (Co, Cr, Mn) the absorption extends well into the visible.

When the sample is irradiated with light in the range 3900–4300 Å, several broad visible absorption bands are introduced, as shown for $SrTiO_3$: Fe, Mo in Fig. 2. The thermal decay rate of the photoinduced state varies widely, depending on both dopant and host material. $SrTiO_3$: Fe, Mo has a thermal decay time of several minutes at 300 °K, whereas singly doped $SrTiO_3$: Fe decays in less than a second. At 77 °K both show little or no thermal decay. The induced absorption may also be bleached with visible light.

We interpret the PC changes in the optical spectra as a light-induced transfer of charge between Fe and Mo centers via the conduction or valence bands.[11] The Fe and Mo originally enter the crystal as Fe^{3+} and Mo^{6+}, respectively. Measurements of the Fe and Mo concentrations by atomic absorption spectroscopy show that the total amount of Fe present is close to the amount of Fe^{3+} present, as estimated from EPR data, and that an approximately equal amount of Mo is incorporated into the crystal. Neither the Fe^{3+} nor the Mo^{6+} have significant optical absorption in the visible except near the band edge. This is shown in Fig. 2 as the difference between the pure $SrTiO_3$ curve and the solid line. After irradiation with approximately 4000-Å light (pumping the Fe^{3+} or Mo^{6+} bands), Fe^{4+} and Mo^{5+} are created. Both these ions have visible absorption, thus leading to the observed photochromism, shown in Fig. 2 as the difference between the dotted line and the solid line. The role of the Mo is that of an electron trap, and the thermal decay of the absorbing state is determined, among other things, by the depth of this trap. When Mo is not present, another defect center acts as an electron trap. In this case, the thermal decay rate is faster and the optical absorption band due to Mo^{5+} is missing.

This charge-transfer process is illustrated in Fig. 3. Three possible methods of excitation are shown, all leading to the same optical final state. We defer to Sec. V a discussion of which of these excitation processes actually take place.

III. EXPERIMENTAL PROCEDURE

The samples used for this study were cut from boules obtained from National Lead. A wide range of dopants and concentrations were used. The concentrations referred to in this paper are given in the weight percent of oxide added to the crystal during growth, e.g., 0.05% Fe means 0.05% by weight Fe_2O_3 added to the $SrTiO_3$ powder. The actual concentration of transition-metal impurities can be as much as five times lower than this nominal concentration for some dopants.

Oxidizing heat treatments were carried out in flowing O_2 at approximately 950 °C for several hours. Reduction was obtained by heating to 700–800 °C for several hours under partial pressure of air, typically 1 mm Hg. Reduction and oxidation can take place at temperature as low as 400 °C indicating a high-diffusion mobility for oxygen vacancies.

Optical spectra were taken on a Cary 14 spectrophotometer sometimes using an uncolored, but otherwise identical, sample in the reference arm. Photochromic coloring was obtained using a focused 500-W high-pressure Hg lamp with a $CuSO_4$ filter and Corning 7-59 or 7-54 blue filters. Bleaching was obtained using the same Hg lamp with a water filter and a Corning 3-70 yellow filter. Measurements were carried our at room-temperature, liquid-nitrogen, and liquid-helium temperatures. Unless otherwise mentioned, the optical-absorption bands did not change significantly with temperature.

EPR data were also taken at all three temperatures. The room-temperature and liquid-nitrogen data were obtained using a Varian 100-KC modula-

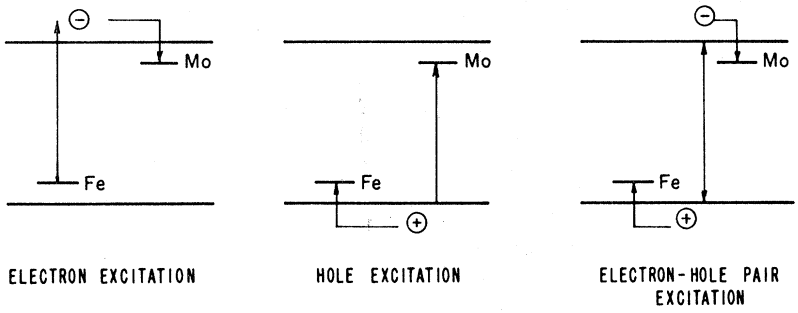

FIG. 3. Schematic diagram of possible charge-transfer mechanisms in PC $SrTiO_3$.

tion spectrometer, whereas for the liquid-helium work a superheterodyne system was employed.

For the EPR-PC studies, the samples were irradiated with light while they were in the microwave cavity. Optical-absorption and EPR measurements were not performed simultaneously although they were frequently performed on the same samples.

IV. EXPERIMENTAL RESULTS

In this section a detailed discussion of the experimental results for the various dopants is presented. In most cases the various optical-absorption bands can be identified as arising from a particular impurity and in a known crystal site and oxidation state. The double doped systems of Ni and Fe co-doped with Mo, which have already been discussed briefly elsewhere,[11,12] will be treated first. Then there follows a detailed treatment of Ni, Fe, and Co singly doped crystals. Finally, other dopants and other host materials will be briefly discussed.

A. $SrTiO_3$: Fe, Mo

In this and following sections only the induced optical-absorption bands will be shown; that is, the intrinsic lattice absorption or any other background absorption will be subtracted out. The PC absorption bands are more easily observed this way.

1. EPR *Spectra*

In $SrTiO_3$: Fe, Mo four principal EPR spectra are observed and all change with light irradiation. Fe^{3+} is observed in both cubic and axial sites. The axial sites are believed to be the Ti^{4+} sites with a nearest-neighbor O^{2-} missing.[15] The oxygen vacancies are necessary to charge compensate the Fe^{3+}. In moderate-concentration $SrTiO_3$: Fe there are equal numbers of cubic and axial sites, as would be expected on the basis of charge compensation if each oxygen vacancy was adjacent to one Fe^{3+} ion (local compensation). In Fe+Mo-doped crystals the number of Fe^{3+} axial sites is less since the Mo^{6+} centers also compensate the Fe^{3+}. These are the only spectra observed in unirradiated crystals. If ~3900–4300-Å or band-gap light is shone on the crystal, both of these spectra decrease and two other spectra appear. On spectum is due to Mo^{5+} in a cubic site[16]; the other spectrum is a holelike center with an isotropic g tensor ($g = 2.0123$) and will be discussed in more detail in the section on $SrTiO_3$: Fe (Sec. V D). Whereas the Mo^{5+} EPR correlates with one of the PC absorption bands observed in $SrTiO_3$: Fe, Mo, and increases as the Fe^{3+} resonance decreases, the same is not necessarily true for the isotropic hole center. Its magnitude depends on the amount of greater than band-gap light incident on the crystal. No EPR center is observed which can be assigned to Fe^{2+} or Fe^{4+}.

2. *Interpretation of the Optical Spectra*

The EPR spectra by themselves are not sufficient to identify which center lost an electron and which center gained an electron. To determine this, the effect of oxidation and reduction of Fe and Mo must be studied. This is shown in Fig. 4. If a crystal doped only with Fe is oxidized by heating to approximately 800 °C in a flowing O_2 atmosphere, two optical-absorption bands are introduced at 4150 and 5850 Å, respectively, as shown in Fig. 4(a). This absorption most likely arises from Fe^{4+} in a cubic site. In a crystal containing $10^{19}/cm^3$ Fe^{3+} ions, only a few percent oxidize to Fe^{4+} as a result of this heat treatment. The above absorption bands are identical to the PC-induced absorption in $SrTiO_3$: Fe, Mo, with the exception that the PC absorption shows an additional band in the long-wavelength region. This latter band can be explained when we examine Fig. 4(b). This shows the effect of reduction on Mo-doped $SrTiO_3$.[17] A band centered at 6500 Å is introduced which can be ascribed to Mo^{5+}. The sum of these two bands add up to produce the PC absorption in $SrTiO_3$: Fe, Mo, as shown in Fig. 4(c). The reduction of $SrTiO_3$: Fe or oxidation of $SrTiO_3$: Mo produce no absorption bands in the visible. The role of the Fe^{3+} axial sites is not clear and will be discussed in the section on $SrTiO_3$: Fe (Sec. IV D). To summarize, it appears likely that for less than band-gap light,

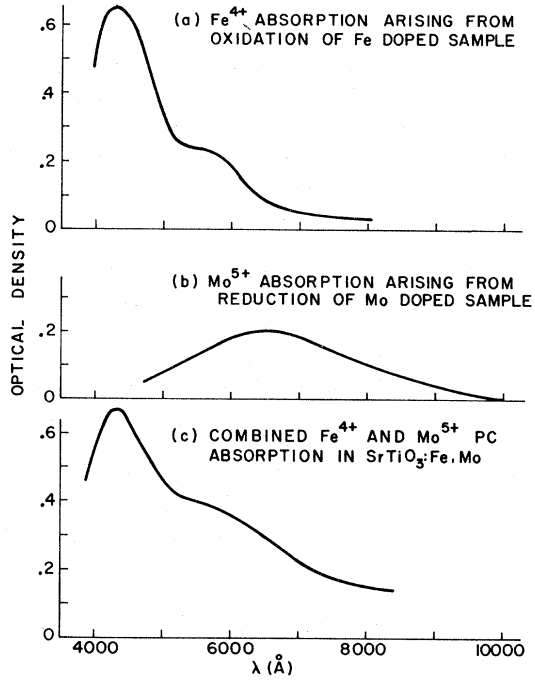

FIG. 4. Optical-absorption bands appearing in (a) $SrTiO_3$: Fe after oxidation, (b) $SrTiO_3$: Mo after reduction, and (c) $SrTiO_3$: Fe, Mo after irradiation with 3900–4300-Å light. Sample thickness = 0.025 cm, T = 77 °K.

electrons are removed from Fe^{3+} cubic sites producing Fe^{4+}, and that these electrons are trapped at Mo^{6+} sites thereby producing Mo^{5+}. The PC absorption is the sum of the absorption bands arising from Fe^{4+} and Mo^{5+}.

B. $SrTiO_3$: Ni, Mo

This material follows the behavior of the Fe + Mo crystals closely. The Mo^{6+} again acts as an electron trap and the Ni centers photo-oxidize under ~ 3900–4300-Å light excitation. However, in this case, the dominant and stable valence state as shown by EPR studies is Ni^{2+} in cubic sites. Presumably some Ni^{2+} in axial sites also exists but would not be observable by EPR because of the high zero-field splitting of the ground state. The induced PC absorption is shown in Fig. 5. After blue-light irradiation (3900–4300 Å) the Ni^{2+} EPR resonance decreases by as much as 25% and a new resonance due to Ni^{3+} appears.[12] An estimate of the number of centers contributing to these two resonances shows that the number of Ni^{3+} centers appearing is equal to the number of Ni^{2+} centers disappearing, at least to within 50%. Some axial Ni EPR spectra are observed, but they do not play an important role if there are approximately equal amounts of Mo and Ni. The Ni^{3+} absorption band peaks at $\lambda \approx 4900$ Å and has about the same 0.8-eV half-width of the large Fe^{4+} band.

C. $SrTiO_3$: Ni

When $SrTiO_3$ is doped with Ni only, it is still strongly photochromic, although there are some differences compared with double doped Ni + Mo. Some of the induced absorption bands are different and the thermal decay at room temperature is much faster than in $SrTiO_3$: Ni, Mo. A new set of traps more shallow than Mo^{6+} are now active, namely, Ni in axial sites. There are many more axial sites as compared with a Ni + Mo-doped sample since oxygen vacancies are necessary for charge compensation.

1. *Optical Spectra*

Ni-doped $SrTiO_3$ is interesting because of the variety of optical-absorption bands and EPR spectra which can be seen. This allows the positive identification of the major optical-absorption bands. A number of crystals with nominal concentrations from 0.05% to 1.0% NiO were studied and their behavior is similar. The optical spectra for untreated, reduced, and oxidized crystals are shown in Fig. 6. Some of the light-induced absorption bands are already present in the heat-treated samples. This is shown in a different way in Fig. 7, where the differential absorption between the heat-treated crystals and the untreated crystals is plotted.

Let us call the two sharp bands introduced by reduction D_1 and D_2 [where $\lambda(D_1) = 4800$ Å and $\lambda(D_2) = 5750$ Å] and the broad band of Fig. 7(b), introduced by oxidation B [where $\lambda(B) = 4900$ Å]. Finally, another band E, which is smaller in intensity, can frequently be seen at $\lambda(E) = 7000$ Å. All of the optical absorption introduced in the visible region can be explained in terms of these bands.

2. EPR *Spectra*

The EPR spectra found in Ni-doped $SrTiO_3$ are shown in Fig. 8. There are four distinct spectra labeled A, B, C, and D. In addition, some small trace impurities of Fe^{3+} are also observed. These four spectra of Ni have been observed before,[18–20]

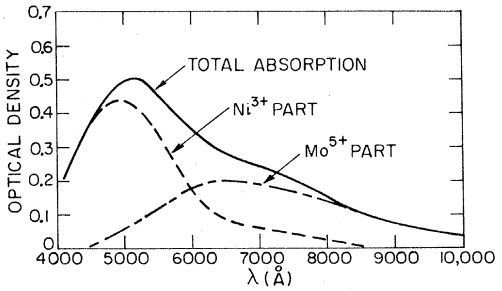

FIG. 5. PC absorption bands in $SrTiO_3$: Ni, Mo. Sample thickness = 0.025 cm, T = 77 °K.

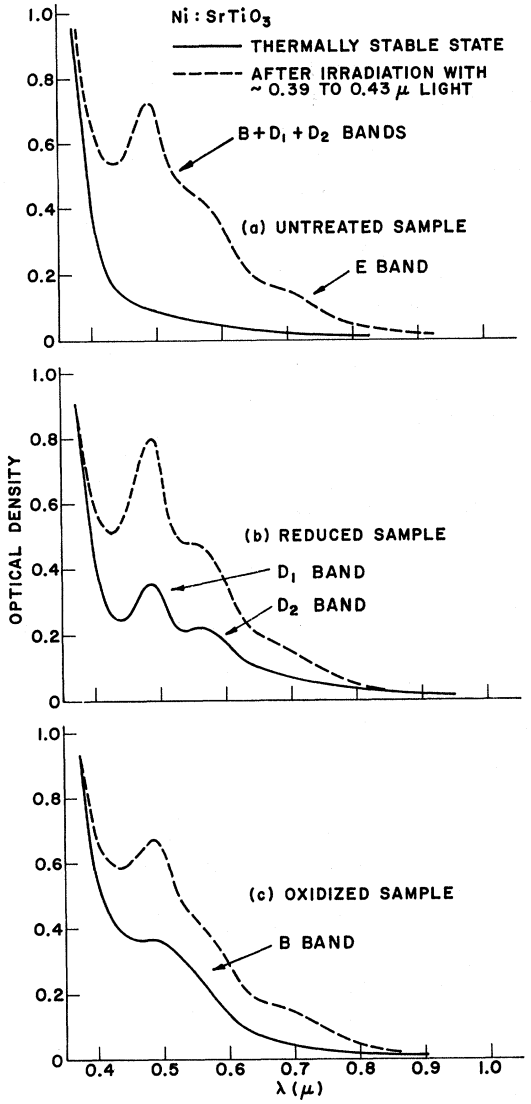

FIG. 6. PC absorption bands in $SrTiO_3$: Ni for (a) untreated, (b) reduced, and (c) oxidized samples. Sample thickness = 0.025 cm, $T = 77$ °K.

and our labeling follows Rubins and Low.[18] We will not discuss the technical EPR aspects of these spectra, but we will only list their identification. All Ni spectra are substitutional on Ti^{4+} sites.

(*a*) Ni^{2+} *in cubic site.* In Fig. 8, the magnitude of the Ni^{2+} spectrum looks small because of the large linewidth (40–80 Oe). Actually, approximately 80% of the observable Ni present is in the form of Ni^{2+} in cubic sites.

(*b*) Ni^{3+} *in cubic site.* This spectrum is absent in reduced samples and increases in oxidized or light-irradiated samples.

(*c*) *and* (*d*) Ni *in axial sites with* [100] *symmetry.* It is assumed that the axial perturbation is caused by the removal of one of the six octahedrally coordinated oxygen ions. The oxygen vacancies must occur because of the requirements of charge compensation. When the compensation is local, a strong axial perturbation on the transition ion results. Off-axis, these sharp lines which can be as narrow as 0.4 Oe break up into complex lines.

Until recently the identity of these two Ni sites was not established. However, it has now been shown[20] that the *C* spectrum comes from a Ni^{3+} ion with a nearest-neighbor oxygen vacancy site, whereas the *D* spectrum arises from a Ni^{3+} ion next to an oxygen vacancy field with two electrons. Our oxidation-reduction experiments are consistent with this interpretation, which now seems to be well established. The center Ni^{3+} next to an oxygen vacancy with one trapped electron, which has a charge state intermediate between the above two centers, is not expected to be observable by EPR because of the large zero-field splitting of the resulting effective $S = 1$ state.[20] We shall label the above-mentioned centers Ni^{3+}-V_O, Ni^{3+}-$V_O(2e)$, and Ni^{3+}-$V_O(e)$, respectively, consistent with the above reference.

We now turn to an interpretation of the EPR and optical spectra for the three different samples. Note that identical crystals were used for the data of Figs. 6–8. The results of the following discussion are summarized in Table I.

3. *Interpretation of Spectra*

(*a*) *Untreated crystal: no light.* There is no optical absorption in the visible and only EPR spectrum *A* is present. Thus, only Ni^{2+} is present in the crystal. The *A* spectrum is cubic Ni^{2+}, but it is assumed that axial Ni^{2+} or, more accurately,[20] Ni^{3+}-$V_O(e)$ is also present. Although Ni^{2+} does not absorb in the visible, its presence does lead to absorption near the band edge and hence to photochromic absorption.

(*b*) *Untreated crystal: blue light.* After irradia-

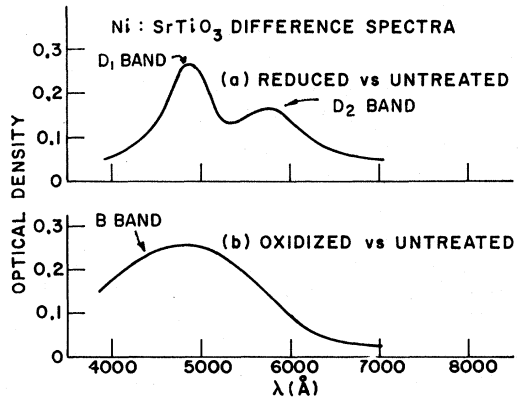

FIG. 7. Absorption bands introduced by heat treatment in $SrTiO_3$: Ni (a) reduced and (b) oxidized.

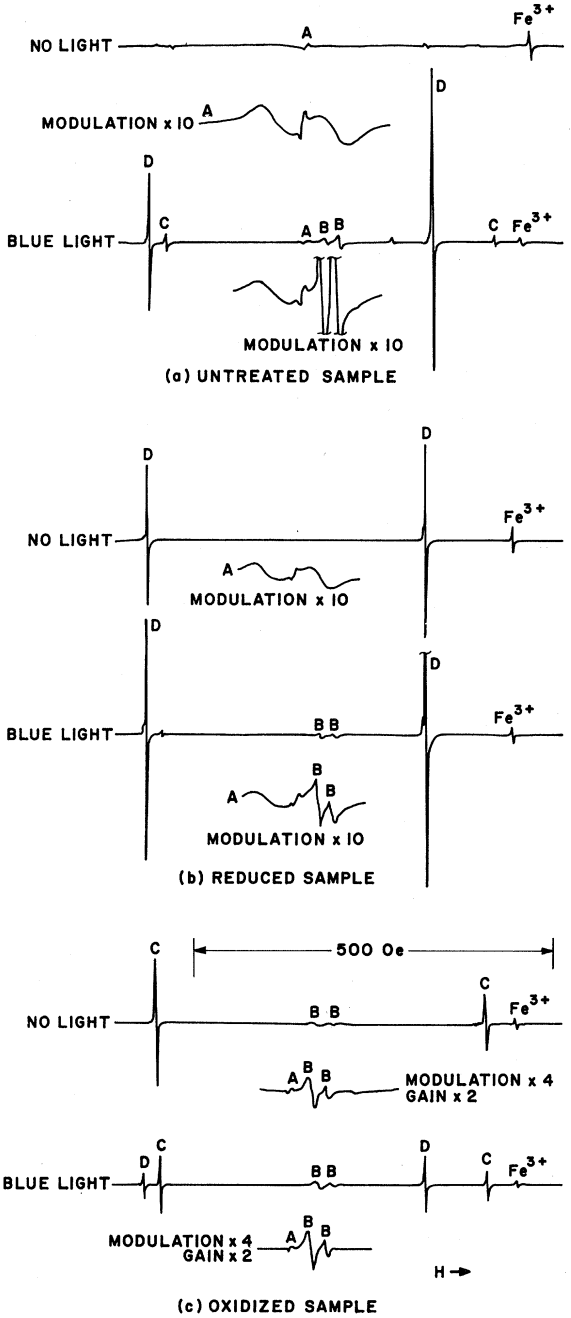

FIG. 8. EPR spectra in $SrTiO_3$: Ni for (a) untreated, (b) reduced, and (c) oxidized samples, with and without coloring light. Sample thickness = 0.025 cm, $T = 77$ °K.

tion with 3900–4300-Å light, optical bands B, D, and E appear. Band E, which is small in magnitude, cannot be explained at this time and will not be discussed further. It is not obvious that the optical absorption in Fig. 6(a) is made up of both B and D bands since B is broad and sits underneath the sharper D bands. However, a consideration of all six cases lends strong support to this assignment. The corresponding EPR spectra for this case show that the Ni^{2+} (A spectrum) has decreased by about 25%, while the cubic Ni^{3+} (B spectrum) and axial Ni^{3+}-$V_O(2e)$ (D spectrum) have come up strongly. The C spectrum Ni^{3+}-V_O is also present but much weaker. We now make the identification B (optical) = B(EPR) and D (optical) = D(EPR). To verify this we must show that the same correspondence holds for the other four cases.

(*c*) *Reduced crystal: no light.* Optically, only the D band is observed, and the EPR spectrum shows the introduction of Ni^{3+}-$V_O(2e)$ sites. This is the expected result of a reduction.

(*d*) *Reduced crystal: blue light.* Figure 8(b) shows that the Ni^{3+}-$V_O(2e)$ spectrum increases further and Ni^{3+} appears as in case of an untreated crystal. Apparently not all the Ni^{3+}-$V_O(e)$ is reduced and blue light has the same effect as in case (b).

(*e*) *Oxidized crystal: no light.* The EPR data show large C and B spectra, e.g., axial Ni^{3+}-V_O and cubic Ni^{3+} as expected from an oxidation treatment. The broad optical band can be associated with the cubic Ni^{3+} sites.[21] No optical absorption which can be correlated with the C spectrum has ever been observed.

(*f*) *Oxidized crystal: blue light.* The B spectrum increases and a small D spectrum also appears. This is consistent with the previous picture. Note that the C EPR spectrum decreases with blue light.

To summarize, we have identified the principal photoinduced optical bands as arising from axial Ni^{3+}-$V_O(2e)$ centers and consisting of two sharp bands of half-width approximately 0.4 eV and peak wavelengths of 4800 and 5750 Å, and cubic Ni^{3+} centers with a peak wavelength of 4900 Å and half-width 0.8 eV.

We conclude by stating that observation of a number of Ni-doped crystals with nominal concentration between 0.05 and 1.0% are all consistent with the assignment given here. Furthermore, rough estimates of the number of centers switched are consistent within a factor of 2 with the optical density changes actually observed.

4. *Line Shapes and Gaussian Curve Fitting*

Since the $SrTiO_3$: Ni optical data are quite complicated with several bands contributing to the observed optical absorption, it is of interest to ask how reliable and unique is the assignment given here. To this end we have attempted to fit a number of experimentally obtained absorption curves to Gaussian line shapes. The results are described below.

The observed PC absorption in $SrTiO_3$: Ni, Mo can be fitted quite well with two Gaussian lines, namely, $\lambda(Mo^{5+}) = 6550$ Å, W (half-width) = 0.80 eV; $\lambda(Ni^{3+}$ cubic) = 4900 Å, $W = 0.80$ eV. A good fit

TABLE I. The PC process[a] in $SrTiO_3$: Ni.

Label in text	*A*		*B*	*C*	*D*
Identification[b]	Ni^{2+}	Ni^{3+}-$V_O(e)$	Ni^{3+}	Ni^{3+}-V_O	Ni^{3+}-$V_O(2e)$
EPR data	$g = 2.20$	not observed	$g_{\parallel} = 2.17$	$g_{\parallel} = 2.03$	$g_{\parallel} = 2.08$
			$g_{\perp} = 2.18$	$g_{\perp} = 2.35$	$g_{\perp} = 2.37$
	linewidth = 50 Oe		linewidth = 2.7 Oe	linewidth = 0.4 Oe	linewidth = 0.4 Oe
Optical absorption	smears band edge	smears band edge	$\lambda(B) = 4900$ Å $W = 0.80$ eV	none observed	$\lambda(D_1) = 4800$ Å $\lambda(D_2) = 5750$ Å $W_1 = W_2 = 0.40$ eV
When observed	Predominant centers in untreated crystal, no light. Decreases with PC switching, oxidation, or reduction.		After PC switching or oxidation	After oxidation, but decreases after PC switching	After PC switching or reduction

[a]PC process: $Ni^{2+} + h\nu$(light) $\rightarrow Ni^{3+} + e$ photo-oxidation; $Ni^{3+} - V_O(e) + e \rightarrow Ni^{3+} - V_O(2e)$ photoreduction,

[b]Definitions: Ni^{2+}, Ni^{2+} in cubic Ti^{4+} ion site; Ni^{3+}. Ni^{3+} in cubic Ti^{4+} ion site; $Ni^{3+} - V_O$, Ni^{3+} in axial site produced by one nearest-neighbor oxygen vacancy; $Ni^{3+} - V_O(e)$, same complex as above with one electron trapped at oxygen vacancy; $Ni^{3+} - V_O(2e)$; same complex as above with two electrons trapped at oxygen vacancy; $h\nu$ = light quantum of approximately 3.0 eV energy; e = conduction-band electron.

has been obtained for a number of crystals with different doping concentration. The Mo^{5+} absorption band fit is further confirmed in reduced $SrTiO_3$: Mo when it is the only absorption band present. The assumption that $SrTiO_3$: Ni, Mo can be fit with only one additional band is further supported by EPR studies which show that cubic Ni^{3+} is the only Ni center which appears after irradiation with 3900–4300-Å light.

The situation is more complicated with $SrTiO_3$: Ni crystals. The first discrepancy is observed in oxidized samples. The optical absorption introduced [Fig. 7(b)] is broader than the cubic Ni^{3+} absorption band. This is shown in Fig. 9(a), where the absorption introduced by oxidation fits the Ni^{3+} cubic band very well for $\lambda > 5000$ Å, but there is additional absorption introduced in the short-wavelength region. All oxidized samples show this behavior as well as most of the PC absorption spectra. Apparently, additional centers are introduced by oxidation. Of course, the EPR data shows that axial Ni^{3+} (*C* spectrum) is also introduced by oxidation, but the EPR spectrum cannot be correlated with the presence or absence of this short-wavelength absorption. Its origin is, at present, unknown.

The peak wavelengths and widths of the *D* spectrum were obtained by curve fitting a number of different crystals and they represent an average value. The linewidths sharpen somewhat at lower temperatures. A typical example is shown in Fig. 9(b). The observed PC absorption is fit to the assumed *B* and *D* spectra. The fit is good, except that additional absorption is observed in the short-wavelength region. The extra absorption at long wavelengths can be well accounted for by another band at $\lambda = 6800$ Å. This band is frequently seen, although it is always small and it cannot be correlated with any EPR spectrum.

D. $SrTiO_3$: Fe

Fe-doped $SrTiO_3$ does not exhibit any PC properties at room temperature, but if cooled to 77 °K, PC changes occur. Apparently, shallow electron traps are available, but the thermal decay time is short (less than 1 sec) at room temperature. The nature of these traps is still somewhat of a mystery because they do not show themselves either in optical absorption or EPR. Nevertheless, the PC changes follow the pattern previously ob-

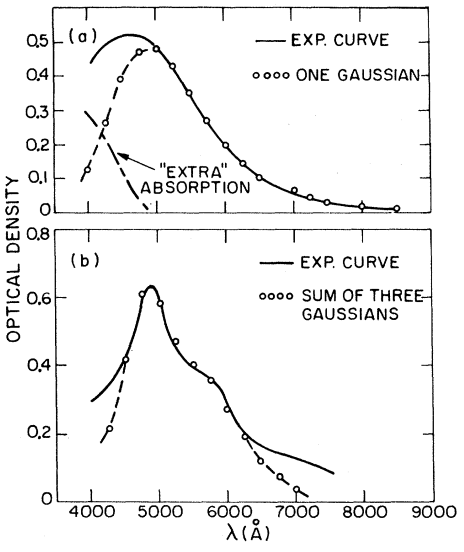

FIG. 9. Gaussian curve fitting of optical-absorption bands in $SrTiO_3$: Ni (a) bands introduced by oxidation and (b) PC bands in untreated sample.

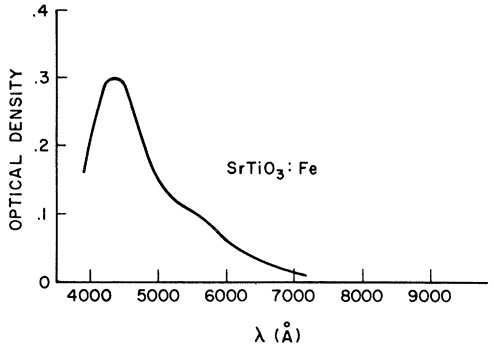

FIG. 10. PC absorption bands in $SrTiO_3$: Fe.

served.

1. EPR *and Optical Results*

The EPR spectra of Fe^{3+} are observed in both cubic and axial sites. For low Fe concentration samples ($< 10^{19}/cm^3$), the amplitudes of both spectra are greatest before light irradiation and decrease after irradiation with blue light. Approximately equal numbers of cubic and axial sites disappear. The induced PC absorption accompanying this change in EPR signal is shown in Fig. 10. It is very similar to the Fe^{4+} spectra obtained by oxidation as shown in Fig. 4(a), as expected from the results with the Fe + Mo-doped crystals. We assume, therefore, that the effect of the blue (less than band-gap) light is to remove an electron from an Fe^{3+} cubic center which subsequently gets trapped. Irradiation with yellow light restores the original condition of the crystal. The observed PC absorption can be approximately fit with two Gaussian absorption bands with peak wavelengths $\lambda_1 = 4250$ Å, $\lambda_2 = 5850$ Å, and half-widths $W_1 = 0.83$ eV, $W_2 = 0.50$ eV.

The role of the axial centers is not clear. Presumably they are either electron donors in analogy to the cubic Fe^{3+} centers or electron traps, as with the axial Ni^{2+} sites. First, consider the latter possibility. This would explain why the same number of cubic and axial Fe^{3+} sites disappear, since one trap is needed for every electron donor. Furthermore, an axial Fe^{3+} center has a net positive charge with respect to the lattice, which would attract an electron. Unfortunately, it has not been possible to prove this interpretation and some difficulties remain.

The lack of a PC effect at room temperature implies a shallow trap in $SrTiO_3$: Fe. However, in lightly doped $SrTiO_3$: Fe, Mo it is possible to see large changes in both the axial and cubic Fe^{3+} EPR spectra at room temperature. In this case, the Fe^{3+} axial spectrum decays more slowly than the PC absorption, which is contrary to expectations for a shallow electron trap. This is illustrated in Fig. 11, where the recovery of the EPR signals and the decay of the PC absorption after illumination with 3900–4300-Å light is shown for a sample containing a low concentration of Fe + Mo. Both Fe^{3+} EPR signals decrease with illumination and recover when the light is removed. These changes are plotted for convenience as positive signals which decrease to zero after sufficient time. All quantities have been normalized to the same arbitrary magnitude at $t = 0$ for easy comparison. The decay of the optical absorption matches perfectly the recovery of the cubic Fe^{3+} EPR signal, as expected. This recovery time is limited by the release of electrons by the Mo^{6+} traps. But, the Fe^{3+} axial signal shows a much slower recovery and even has a slight increase in the first 20 sec before decaying to zero.

The assumption that the axial Fe^{3+} center is another electron donor also encounters difficulties. They are the following: (i) An axial Fe^{4+} center would be expected to have a PC absorption band just as cubic Fe^{4+} does. (ii) In the recovery process, shown in Fig. 11, which takes place after the blue light is turned off, the doubly charged axial Fe^{4+} center should trap electrons more strongly than cubic Fe^{4+}, which contradicts the slow recovery of the axial Fe^{3+} signal.

Another observation adds to the complexity. As the concentration of Fe increases beyond the 0.05% level, the axial Fe^{3+} EPR signal changes in a regular fashion and continues to correlate with the changes in optical absorption. But, the Fe^{3+} signal changes sign from an initial decrease (implying an increase in Fe^{4+} centers) to an increase. Perhaps

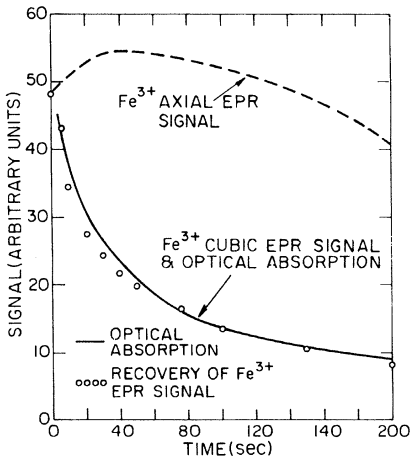

FIG. 11. Comparison of the decay of the PC optical absorption at $\lambda = 5000$ Å and the change in Fe^{3+} EPR signals for a $SrTiO_3$: Fe, Mo sample at room temperature. Magnitude of the cubic Fe^{3+} EPR signal and the PC optical density change are set equal to each other at $t = 0$.

at a higher concentration some Fe^{2+} is present in the crystal so that the process $Fe^{2+} \rightarrow Fe^{3+}$ is possible. Again, one is hampered by lack of EPR data from making any definite conclusions. Bhide and Bhasin[22] have observed both Fe^{3+}-V_O and Fe^{2+}-V_O sites by Mössbauer spectroscopy, although the latter appears only after reduction.

2. *Isotropic* EPR *Center*

We have long observed[10,11,23] a new EPR center which occurs only in PC $SrTiO_3$:Fe. This center has a completely isotropic EPR spectrum down to 1.5 °K. The g value is $g = 2.0123$, which suggests a holelike center.

This spectrum and a similar Al-associated spectrum have recently been studied by Ensign and Stokowski.[24] These authors studied nominally pure and Al-doped $SrTiO_3$, although all their crystals contained trace impurities of Fe. The Al-associated EPR resonance shows a hyperfine structure characteristic of Al^{3+} and they ascribe this center, whose g value is almost identical to the one we observe, to a trapped hole shared by six oxygen ions which surround the Al^{3+} impurity center. The Al^{3+} impurity ion is subsitutional on a Ti^{4+} site and acts as an attractive center for the hole. They do not identify the hole center under discussion now, which they label X-O^-, in analogy with the Al-associated center. The possibility that this center is associated with an iron impurity is discussed, but the experiments do not favor this possibility.

Recent work,[25] which postdates the first writing of this paper, has shown quite unambiguously that this EPR center is due to Fe^{5+}. We will not discuss here the identification of this center, but describe some experimental observations which have a bearing on the PC effect.

The spectrum is usually observed after irradiation with uv light and can be correlated with the wavelength of light used to irradiate the crystal. In addition, an optical-absorption band can be correlated with the magnitude of this EPR line. This is shown in Fig. 12, where the PC absorption observed in a crystal containing 0.01% Fe was studied. If a Corning 7-59 filter is used in conjunction with a Hg lamp for irradiation, then curve (a) results. This has the "normal" shape which we associate with Fe^{4+}. If a series of filters are used consecutively, which increasingly cuts out more of the visible and allows more uv through (e.g., Corning 7-59, 7-54, 7-37), the absorption peak shifts to longer wavelengths and changes character. In Fig. 12, curve (b) shows this effect. This shift is a result of a new band which is introduced by greater than band-gap radiation. This is more clearly seen in curve (c), which is curve (a) subtracted from curve (b). Curve (d) cuts off even more of the effect of the Fe^{4+} absorption and shows the new band more clearly.

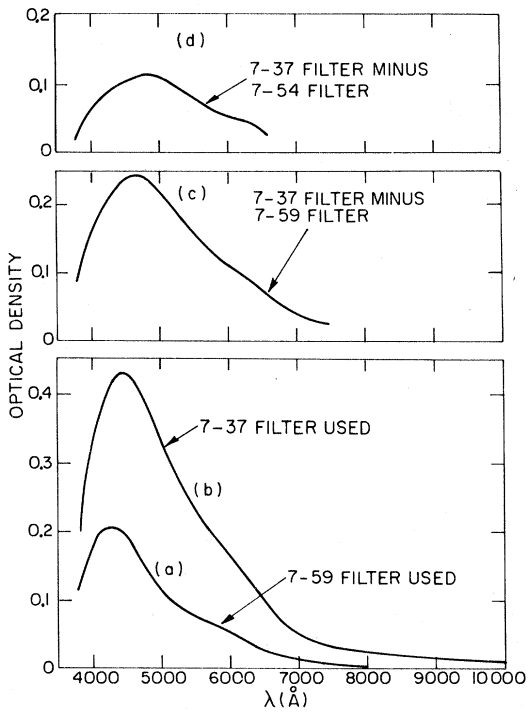

FIG. 12. Effect of greater than band-gap light on the PC absorption bands in $SrTiO_3$:Fe. Curve (a), sample colored through 7-59 filter (sub-band-gap light). Curve (b), sample colored through 7-37 filter after being colored with 7-59 filter (incremental change results from both sub-band-gap and greater than band-gap light). Curve (c), incremental effect of 7-37 filter after sample previously colored with 7-59 filter. Curve (d), incremental effect of 7-37 filter after sample previously colored with 7-54 filter.

The EPR data supports this conclusion. Initially, if a 7-59 (mainly sub-band-gap light) filter is used, Fe^{3+} cubic and axial spectra decrease by equal amounts and very little or no hole-center spectrum is observed. As the sequence of filters 7-59, 7-54, and 7-37 are consecutively placed in front of the irradiating light, the successive changes in Fe^{3+} EPR spectrum becomes progressively less, so that in going from the 7-54 to 7-37 filter, practically no change is observed. The opposite effect is obtained for the isotropic hole center. It is hardly excited with a 7-59 filter, but it increases greatly with the 7-54 filter and increases still more with the 7-37 filter. This shows that the hole center is created by greater than band-gap light but not by sub-band-gap light.

A consistent picture then is the following: With sub-band-gap light, electrons are removed from Fe^{3+} centers to produce Fe^{4+} and an electron in the conduction band which becomes trapped at some unknown electron trap, possibly the Fe^{3+} axial center.

On the other hand, greater than band-gap light creates electron-hole pairs. The electrons are trapped as before and the holes are trapped at hole traps which, based on the results of Ref. 24, must be Fe^{4+}, giving rise to the isotropic EPR line.

The new absorption band introduced with band-gap light and which peaks at around 5000 Å is probably the same one observed by Ensign and Stokowski[24] along with the isotropic hole center. However, they find that in $SrTiO_3$: Al the hole center increases by a factor of 50, whereas the 5000-Å band remains unchanged. They conclude therefore that the absorption band does not arise from the isotropic hole center.

E. $SrTiO_3$:Co

Many complex Co bands can be introduced by heat treatment of Co-doped $SrTiO_3$, but that will not be discussed here. The PC changes appear to be simple and fit into the picture already developed. The induced PC absorption is shown in Fig. 13 and is the same as the bands introduced by oxidation.

On the basis of EPR and heat treatment experiments, it is concluded that most of the Co enters the crystal as Co^{3+}. Upon uv irradiation, an electron is removed from the cubic Co^{3+} to produce Co^{4+}. This electron is then trapped by a cubic Co, thereby creating cubic Co^{2+} sites. We therefore have

$$2Co^{3+}(\text{cubic}) \underset{h\nu}{\rightarrow} Co^{4+}(\text{cubic}) + Co^{2+}(\text{cubic}) .$$

Bleaching with visible light or thermal decay will return the Co center to the 3+ state. This is similar to $SrTiO_3$: Ni, where the Ni can act as both electron donor and electron trap. In this case,

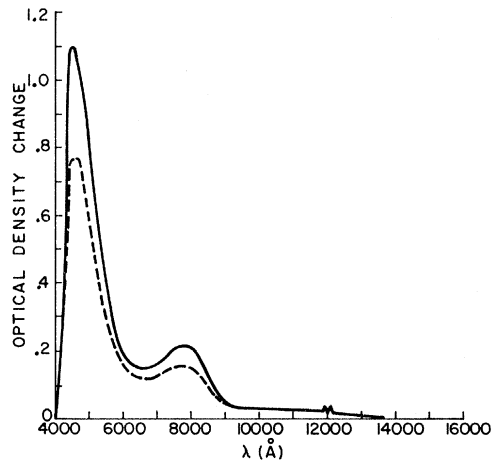

FIG. 13. PC absorption bands in $SrTiO_3$:Co. Dotted line, 78 °K; solid line, 4.2 °K. Sample thickness 0.010 in.

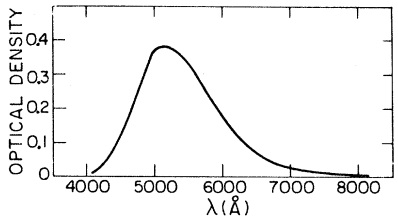

FIG. 14. PC absorption bands in $SrTiO_3$:Cr.

however, the identical center acts as donor and trap.

The evidence for the PC process in $SrTiO_3$: Co is more indirect than it was for Ni doping. Co^{3+} cannot be observed by EPR[19] nor directly identified by optical absorption. Nevertheless, it is clear that Co is present in the crystal by its effect on the optical absorption near the band edge. After uv irradiation, the PC bands introduced are identical to those produced by oxidation, and from this we infer the PC photooxidation process $Co^{3+} \rightarrow Co^{4+}$. On the other hand, accompanying the PC changes in optical absorption, the creation of a Co^{2+} cubic EPR spectrum is observed.[16] The spectrum is not normally present in an untreated crystal but can also be introduced by a mild reduction, again supporting the belief that the Co is originally present as Co^{3+}.

F. Other Transition Metals: Cr, V, Mn

Other transition metals have been found to be photochromic in $SrTiO_3$. For example, Cr-doped $SrTiO_3$ is strongly PC. The Cr initially enters as Cr^{3+} and the crystal is red in color. Oxidation studies suggest that the PC change shown in Fig. 14 is once again

$$Cr^{3+} \underset{h\nu}{\rightarrow} Cr^{4+} ,$$

although this material has not been studied as thoroughly as the previously mentioned dopants. Vanadium also shows a slight PC effect, whereas Mn-doped $SrTiO_3$ does not change at all with light. This is probably because the stable form of Mn in $SrTiO_3$ is Mn^{4+}. If the same photo-oxidation took place, Mn^{5+} would result, which is probably not stable.

Finally, various combinations of transition-metal ion dopings are possible, leading to more complex absorption bands. We mention, for example, $SrTiO_3$: Ni, Co, which is found to have a strong PC absorption and a long thermal decay time at room temperature.

G. Other Titanates: TiO_2 and $CaTiO_3$

$CaTiO_3$ doped with transition metals has PC properties very similar to $SrTiO_3$. The slight dif-

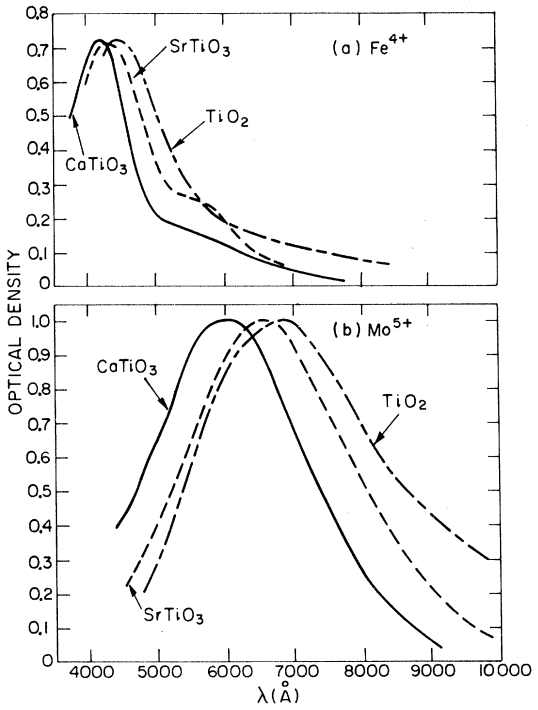

FIG. 15. Effect of band gap on the Fe^{4+} and Mo^{5+} absorption bands in $CaTiO_3$, $SrTiO_3$, and TiO_2. Data taken at room temperature, except for the TiO_2: Fe^{4+} curve which was obtained at 77 °K. Peak absorption for each titanate was set equal for ease of comparison.

ferences are a result of the slightly larger bandgap, 3.4 eV rather than 3.2 eV. As a result of this, the electron trap depths are all somewhat deeper, leading to increased thermal lifetimes for a given impurity ion in $CaTiO_3$ as compared with $SrTiO_3$. Single-crystal TiO_2, which has a smaller bandwidth (3.0 eV) than $SrTiO_3$, does not show any appreciable photochromism at room temperature. However, at 77 °K and lower it shows PC properties similar to the alkali earth titanates. This is because the properties of the TiO_6 molecular complex appear to be the most important element for photochromism in the titanates.

The effect of the bandgap on the Fe^{4+} and Mo^{5+} optical-absorption bands is shown in Fig. 15. The Fe^{4+} curves were obtained by oxidation of Fe-doped titanates, with the exception of the TiO_2 curve which was obtained from the induced PC absorption bands. It proved impossible to oxidize the TiO_2: Fe by the same technique used for $SrTiO_3$ and $CaTiO_3$. The Mo^{5+} bands were obtained by reduction of the appropriate titanate. The shift to shorter wavelengths with increasing band gap is apparent. Another effect of changing the bandgap is that the material with the largest band gap also shows the largest PC absorption changes for a given impurity ion. The effect, which is not shown in Fig. 15 because the absorption peaks are normalized, is about 20% in going from $SrTiO_3$ to $CaTiO_3$. It probably arises because there is less overlap between coloring and bleaching light so the photo-oxidation process can be driven further before the dynamic equilibrium determined by photobleaching sets in.

V. NATURE OF PC EXCITATION AND ABSORPTION BANDS

Unfortunately, detailed knowledge about the nature of the photochromic absorption is lacking. It seems to be a charge-transfer type of process similar to the fundamental band-gap absorption. In addition,

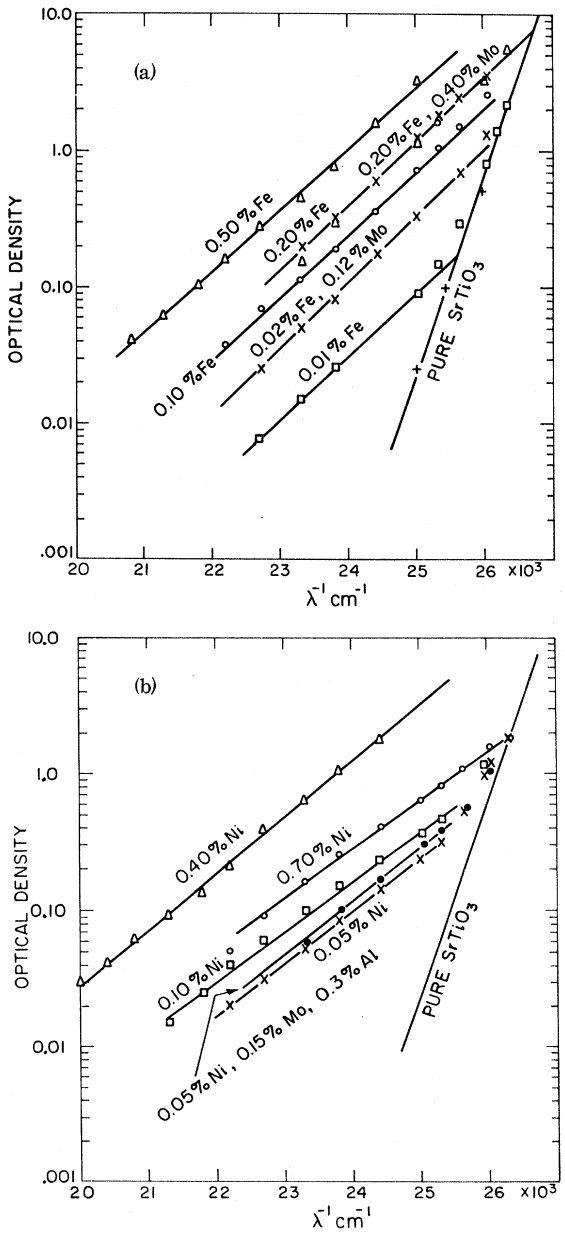

FIG. 16. Absorption near the band edge in (a) $SrTiO_3$: Fe and (b) $SrTiO_3$: Ni.

the absorption can be associated with a particular ion and oxidation state.

A. Coloration Process

The absorption arising from the transition ion in its thermally stable state appears as a smearing out of the fundamental band-edge absorption. This makes it difficult to study this absorption in detail. Nevertheless, this region becomes clearer if we plot the optical absorption as shown in Fig. 16. Here the optical density is plotted on a log scale vs the reciprocal wavelength for both Fe- and Ni-doped crystals of varying concentrations. In this type of plot the fundamental edge absorption of $SrTiO_3$ is a straight line.[26] This is known as Urbach's law and is obeyed by many insulators and semiconductors. Note that the extra absorption introduced in the visible by the transition-metal impurity follows a similar law, but with a considerably reduced slope. Furthermore, for a given wavelength the amount of absorption is proportional to the concentration of impurity over a range of greater than 3:1. The concentrations given in the figures are nominal concentrations, and the actual relative concentrations could be in error by a factor of 2. Such a plot is probably the most accurate method of measuring relative concentrations of different samples. In Fig. 16(b), the 0.70% Ni curve falls below the 0.40% Ni curve, which is the only anomaly and probably means that the actual concentration of this sample is much lower than the nominal concentration.

To obtain such curves it is necessary for all the transition ions to be in the same oxidation state. Otherwise the absorption from the other oxidation states will alter the experimental data in the region where they absorb. Two Fe+Mo-doped crystals and one Ni+Mo-doped crystal are included, and they behave as would be predicted by their transition-metal concentration above, regardless of their Mo concentration. It is the extra absorption in the visible shown in Fig. 16 which gives rise to the PC charge-transfer process.

The similarity of these curves to the pure $SrTiO_3$ absorption suggests a similar mechanism. Two possibilities may be considered: (i) An electron is excited directly from the Fe^{3+} site, for example, into the conduction band, or (ii) the six O^{2-} ions surrounding the Fe^{3+} ions have their energies raised by the proximity of the Fe^{3+} ion. Then a charge transfer may occur between one of these ions and their neighboring Ti ions, leading to an absorption similar to, but lower in energy than, the fundamental edge absorption. We cannot distinguish between the two processes without further experimental work, although the latter one seems more attractive.

B. Photochromic Absorption

The most striking feature about the PC absorption bands is the high oscillator strength. This quantity can be estimated using Smakula's equation[27] which is

$$Nf = 0.87\times10^{17}[n/(n^2+2)^2]\,k_{\max}W\,,$$

where N is the number of absorbing impurity centers per cm^3, f is the oscillator strength, n is the index of refraction of the material (2.4 for $SrTiO_3$), $k_{\max}$ is the peak absorption coefficient of the absorption band in cm^{-1}, and W is the half-width of the absorption band expressed in eV. $k_{\max}$ and W are obtained from the optical data. N can be estimated from the EPR data. We obtain

$$f_{Fe^{4+}}\approx 0.4,\quad f_{Ni^{3+}}\approx 0.25,\quad f_{Mo^{5+}}\approx 0.1\,.$$

These values are only approximate. Nevertheless, the values obtained are almost as large as those observed for F centers[10] and much greater than would be expected, for example, from internal electronic d-d transition-metal ions in insulators.

A possible process which could have such a high oscillator strength is the one leading to the fundamental band-gap absorption, that is, a transition between an O^{2-} p state and a Ti^{4+} d state which is allowed, and where the overlap between the two

TABLE II. Summary of photochromic processes in transition-metal-doped $SrTiO_3$.

Impurity ions	Photo-oxidation	Photoreduction	Method of observation: EPR	Method of observation: Optical
Fe, Mo	$Fe^{3+}\rightarrow Fe^{4+}$	$Mo^{6+}\rightarrow Mo^{5+}$	Fe^{3+}, Mo^{5+}	Fe^{4+}, Mo^{5+}
Ni, Mo	$Ni^{2+}\rightarrow Ni^{3+}$	$Mo^{6+}\rightarrow Mo^{5+}$	Ni^{2+}, Ni^{3+}, Mo^{5+}	Ni^{3+}, Mo^{5+}
Fe	$Fe^{3+}\rightarrow Fe^{4+}$	unknown [possibly Fe^{3+}-$V_O\rightarrow Fe^{3+}$-$V_O(e)$]	Fe^{3+}, Fe^{3+}-$V_O(e)$	Fe^{4+}
Ni	$Ni^{2+}\rightarrow Ni^{3+}$	Ni^{3+}-$V_O(e)\rightarrow Ni^{3+}$-$V_O(2e)$	Ni^{2+}, Ni^{3+}, Ni^{3+}-V_O, Ni^{3+}-$V_O(2e)$	Ni^{3+}, Ni^{3+}-$V_O(2e)$
Co	$Co^{3+}\rightarrow Co^{4+}$	$Co^{3+}\rightarrow Co^{2+}$	Co^{2+}	Co^{4+}
Cr	$Cr^{3+}\rightarrow Cr^{4+}$	unknown	Cr^{3+}	Cr^{4+}
Mn, V	no significant PC effect		Mn^{4+}	

TABLE III. Room-temperature decay times of PC titanates.

Impurity ions	$SrTiO_3$	$CaTiO_3$
Fe	<1 sec	<1 sec
Ni	20 sec	20 sec
Fe, Mo	1 min	5 min
Ni, Mo	1 min	6 min
Co	3 min	2 h
Ni, Co	2 h	not measured

ions can be expected to be large, say 10%. In fact, if one applied Smakula's equation to the large absorption band of $SrTiO_3$ in the uv as determined by Cardona,[28] one obtains

$$N \approx 3\times10^{22}, \quad k \approx 8\times10^{5}\ \mathrm{cm}^{-1}, \quad W \approx 2.5\ \mathrm{eV},$$

giving $f \approx 0.2$ a value close to what we find for the transition-metal ions.

A possible process having the desired characteristics is a charge-transfer transition of an electron from a nearest-neighbor oxygen to the transition metal. Such a process has been suggested recently to explain the large visible absorption band introduced by Cu in ZnS.[29] Again, the experimental data are not conclusive and this question must await a more detailed study.

VI. CONCLUSIONS

In this section we shall review the results obtained on the PC effect in transition-metal-doped $SrTiO_3$. The model is the same for all transition elements, namely, the photoexcitation and subsequent transfer of an electronic charge from one impurity center to another. Whether the mobile charge is actually an electron or a hole is not determined in these experiments. The photon energy required is somewhat below the band-gap energy. However, greater than band-gap light produces electron-hole pairs which can also lead to a PC effect. The PC absorption bands introduced in the visible region are believed to be charge-transfer bands associated with the relevant transition-metal ions. Doping with different ions modifies such things as the position of the absorption bands, quantum efficiency of coloring and bleaching, and thermal decay rates, but the basic mechanism remains the same.

A summary of the various impurity complexes important in the PC effect is shown in Table II. Some cases are better understood than others, usually because of the existence of enough EPR spectra to make a proper identification. The Ni-doped systems are outstanding in this respect. In contrast, the photoreduction process in Fe-doped crystals is not yet understood.

The thermal decay times of various PC titanates may be of interest, especially for potential applications. Table III lists these times for some of the materials studied. The times shown in the table are the times for the optical absorption to decrease to one-half its original value for some typical samples. These times should be regarded as only approximate since the actual thermal decay depends on many factors such as impurity concentration and the number of centers switched. Nevertheless, a wide spread in decay time is found with the longest lived samples decaying to half their original coloration in several hours. These latter crystals, if kept in the dark, will have considerable coloration after several weeks since the decay rate becomes progressively slower as the absorption bands decrease.

Several unresolved problems remain. We have already mentioned the photoreduction step in $SrTiO_3$: Fe. Many complex bands were observed in Co-doped crystals which were not discussed here since they have yet to be identified. It has not been determined whether electron or hole motion is responsible for the charge transfer. The question of quantum efficiency for coloring and bleaching has not been studied in any detail. Finally, a theory which would predict the nature and position of the PC bands would be very desirable.

ACKNOWLEDGMENTS

I would like to acknowledge many helpful discussions with, and encouragement from, Dr. Z. Kiss. Also, numerous discussions with Professor P. Pershan of Harvard University and Professor D. McClure of Princeton University were very helpful, especially concerning the nature of the photochromic mechanism. The experimental work profited from the very able assistance of R. Nielson.

†Research sponsored by the Defense Atomic Support Agency (DASA), Washington, D.C., under contract No. DASA-01-68-C-0064.

[1]G. H. Brown and W. G. Shaw, Rev. Pure Appl. Chem. 11, 2 (1961).

[2]R. Dessaver and J. P. Paris, *Advances in Photochemistry* (Interscience, New York, 1963), Vol. 1, pp. 275–322.

[3]R. Exelby and R. Grinter, Chem. Rev. 65, 247 (1965).

[4]Z. J. Kiss, Phys. Today 23, 42 (1970).

[5]Brian W. Faughnan, David L. Staebler, and Zoltan J. Kiss, *Applied Solid State Science* (Academic, New York, 1971), Vol. 2, pp. 107–172.

[6]D. B. Medved, Am. Mineralogist 39, 615 (1954).

[7]R. K. Swank, Phys. Rev. 135, A266 (1964).

[8]H. Pick, Ann. Physik 31, 365 (1938).

[9]H. Pick, Ann. Physik 37, 421 (1940).

[10]J. J. Markham, *F Centers in Alkali Halides* (Academic, New York, 1966).

[11]B. W. Faughnan and Z. J. Kiss, Phys. Rev. Letters

21, 1331 (1968).
[12]B. W. Faughnan and Z. J. Kiss, IEEE J. Quantum Electron. QE-5, 17 (1969).
[13]Z. J. Kiss and W. Phillips, Phys. Rev. 180, 924 (1969).
[14]L. Rimai and G. A. de Mars, Phys. Rev. 127, 702 (1962).
[15]E. S. Kirkpatrick, K. A. Müller, and R. S. Rubins, Phys. Rev. 135, A86 (1964).
[16]B. W. Faughnan (unpublished).
[17]The $SrTiO_3$:Mo crystal has some Al^{3+} added to compensate the Mo^{6+}. Otherwise, the Ti lattice will reduce, thereby producing conduction electrons. The optical absorption of the conduction electron would make the observation of the Mo^{5+} band difficult.
[18]R. S. Rubins and W. Low, in *Proceedings of the First International Conference on Paramagnetic Resonance, Jerusalem*, 1962, edited by W. Low (Academic, New York, 1963), pp. 59–67.
[19]W. Low and E. L. Offenbacher, *Solid State Physics*, Vol. 17 (Academic, New York, 1965), p. 136.
[20]K. A. Müller, W. Berlinger, and R. S. Rubins, Phys. Rev. 186, 361 (1969).
[21]See discussion of line shapes below.
[22]V. G. Bhide and H. C. Bhasin, Phys. Rev. 172, 290 (1968).
[23]B. W. Faughnan and Z. J. Kiss, Bull. Am. Phys. Soc. 12, 642 (1967).
[24]T. C. Ensign and S. E. Stokowski, Phys. Rev. B 1, 2799 (1970).
[25]K. A. Müller, Th. von Waldkirch, W. Berlinger, and B. W. Faughnan, Solid State Commun. (to be published).
[26]M. I. Cohen and R. F. Blunt, Phys. Rev. 168, 929 (1968).
[27]D. L. Dexter, *Solid State Physics*, edited by F. Seitz and D. Turnbull, Vol. 6 (Academic, New York, 1958).
[28]Manuel Cardona, Phys. Rev. 140, A651 (1965).
[29]I. Broser, K. H. Franke, and H. J. Schulz, in *Proceedings of the International Conference on Semiconductors*, edited by D. G. Thomas (Benjamin, New York, 1967), p. 81.

PHYSICAL REVIEW B VOLUME 4, NUMBER 10 15 NOVEMBER 1971

Velocities of Sound in Polycrystalline Neon†

R. Balzer,* D. S. Kupperman, and R. O. Simmons
Department of Physics and Materials Research Laboratory, University of Illinois, Urbana, Illinois 61801
(Received 26 July 1971)

The longitudinal and transverse velocities of sound have been measured in polycrystalline specimens of neon from 18 to 24.5 K by ultrasonic pulse-echo techniques. The results are compared to values at lower temperatures obtained previously by Batchelder and co-workers and by Bezuglyi and co-workers. From these results the isothermal compressibility has been calculated. Comparisons made with various model calculations show the data to be in best agreement with the improved self-consistent model calculations of Goldman, Horton, and Klein.

Noble-gas crystals have been the subject of extensive theoretical as well as experimental investigations during the past several years. The heavier gases such as argon and krypton may be taken as almost ideal examples for studying calculations of lattice theory. A great deal of experimental data for these crystals are already available. For helium, the lattice dynamics are dominated by effects arising from large zero-point motion, affecting many of the macroscopic features of solid helium. Neon represents an intermediate case, and zero-point motion is supposed to have only an intermediate influence in the dynamical description of the solid.

For solid neon, the measured thermodynamic properties, particularly the bulk modulus, have been uncertain in the upper third of its temperature range before melting. The only elastic measurement reported above 20 K, where the most rapid temperature variation is expected to occur, is a value for the bulk modulus obtained by Batchelder and co-workers from x-ray isobaric lattice thermal expansion of crystals at pressures of 0 and 8 bar (800 kN m^{-2}), respectively.[1] At 20 K the measured relative change in lattice parameter between 8 and 0 bar was about $(4.5 \pm 0.5) \times 10^{-4}$. When one compares this to the value of the coefficient of linear thermal expansion, about 13×10^{-4} deg^{-1} near 20 K, one sees that temperature differences of order 20 mdeg could contribute the majority of the uncertainty.

Because the high-temperature region is a particularly sensitive test of lattice models, and because large experimental uncertainty exists there, further independent measurements are desirable. Polycrystalline specimens are easiest to prepare, but they exhibit considerable grain growth and suffer easy plastic deformation at high temperatures. This renders measurements somewhat variable, and the present work is no exception, but these disadvantages have been somewhat overcome here by the use of many specimens.